

Effect of V and C on the hot flow behavior of V microalloyed steels

Hai-lian Wei¹, Guo-quan Liu^{1,2}

¹ School of materials science and engineering, University of Science and Technology Beijing,
Beijing 100083, China

² State Key Laboratory for Advanced Metals and Materials, University of Science and Technology
Beijing, Beijing 100083, China

Key words: V microalloyed steels; hot deformation; constitutive equations; dynamic recrystallization

INTRODUCTION

Vanadium microalloyed steels have been studied and used widely, such as in oil, automobile and other machinery industry [1,2]. The wide applicability of such type of steel is based on the fact that they do not require heat treatment after they are shaped into parts. So an important saving of costs, energy and time can be achieved [3]. In order to improve the properties of this material, the parameters of the forming process must be controlled carefully.

Different factors including the chemical composition may alter the flow behavior during the hot deformation of metals, among them V and C are two important alloy elements. There have already been some researches regarding the effect of V and C on the hot deformation behavior of steels. Medina et al. [4,5] indicated that V addition in low carbon steels had a hardening effect on the austenite and can increase the peak strain. Wu et al. [6] found that the addition of V and Ti in Nb microalloyed steels can retard the dynamic recrystallization (DRX) kinetics.

The C content has a complex effect and there is still disagreement regarding the effect of C content on the hot deformation of steels. Wray [7] reported that increasing the C content decreased the flow stress of carbon steels. Medina et al. [4] found that the peak stress of carbon steels decreased with the increase of C content. Beladi et al. [8] found that C appeared to not have any specific effect on the stress-strain behavior of Nb microalloyed steels. Some reports [9,10,11] showed that increasing the C content reduces the flow stress at high temperatures and low strain rates, but increasing the C content increases the flow stress at low temperatures and high strain rates.

To date, research has mainly focused on the effect of C on hot deformation of plain carbon steels, and few results have been reported for microalloyed steels. In microalloyed steels, C interacts with microalloying elements (e.g., V), affecting the hot deformation behavior. So the aim of this work is to clarify the effect of V and C on hot flow behavior of V microalloyed steels during the hot compression deformation. The findings of this study can serve as reference for further research.

EXPERIMENTAL MATERIAL AND PROCEDURE

The chemical composition of the steels used in this investigation is given in Table 1.

Table 1 Chemical composition of the experimental steels (wt%)

Steels	C	Mn	Si	V	S	P	Al	N
A	0.36	1.42	0.27	—	0.0045	0.0053	≤0.005	0.0045
B	0.37	1.46	0.38	0.089	0.0042	0.0058	≤0.005	0.0071
C	0.055	1.45	0.38	0.080	0.0030	0.0057	≤0.005	0.0073

The experimental steels were melted and casted into an ingot of 50 kg in vacuum induction furnace, hot forged into rods. Samples of $\Phi 8 \times 15$ mm were cut off from the rods. To determine the soaking temperature that solutionizes the vanadium prior to deformation testing, the following equations were used [12]. Table 2 gives the solution temperatures calculated for the two vanadium microalloyed steels used in this study.

$$\log[V][C]=-9500/T+6.72 \quad (1)$$

$$\log[V][N]=-8330/T+3.40 \quad (2)$$

Table 2 Calculated solution temperatures of the steels

Steels	Temperature of solubility of VC (°C)	Temperature of solubility of VN (°C)
B	885	989
C	774	983

The compression tests were carried out on a Gleeble-1500 thermo-mechanical simulator in the temperature range from 900 °C to 1100 °C at an interval of 50 °C and at constant true strain rates of 0.005, 0.01, 0.1, 0.5, 1 and 10 s⁻¹, respectively. Prior to the compression, specimens were heated in vacuum at the rate of 10 K/s to 1150 °C for 5 min. From Table 2 it is seen that vanadium in both steels can be completely dissolved at 1500 °C. Then all specimens were cooled to the deformation temperature with the cooling rate of 6.7 K/s and kept at the test temperature for 30 s before compression. Specimens were deformed to a strain of 1.0, then they were water quenched immediately to room temperature.

RESULTS AND DISCUSSION

True stress and true strain

Fig. 1 and Fig. 2 show the stress-strain curves of the experimental steels deformed at different temperatures and strain rates. It can be found that the flow stress increases with the decrease of temperature and the increase of strain rate, steels exhibit a typical DRX behavior under higher temperatures and lower strain rates, while at lower temperatures and higher strain rates, the shape of true stress-true strain curve resembles typical dynamic recovery (DRV) behavior.

It can be found from Fig. 1 that under the same hot deformation conditions, the flow stress of the steel A is lower than the steel B, which indicates that V addition in steels can effectively increase the flow stress.

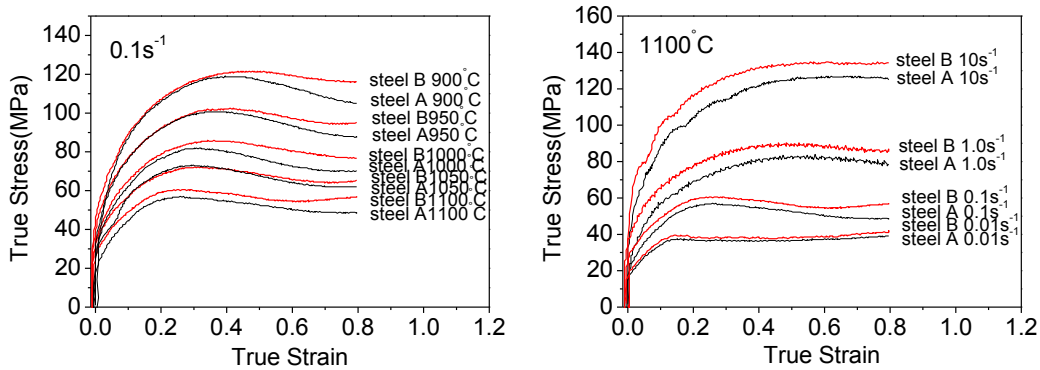


Fig. 1 Flow curves of steel A and steel B obtained at: (a) 0.1 s⁻¹; (b) 1100 °C.

From Fig. 2 it can be seen that at lower strain rates (0.005 and 0.1 s⁻¹), the steel C has a higher flow stress than the steel B. However, when the strain rate increases to 1 and 10 s⁻¹, the steel B shows higher flow stress than the steel C. It demonstrated that C addition in vanadium microalloyed steel has a softening effect at lower strain rates, but a hardening effect at higher strain rates. The reasons for this trend are explained in detail below.

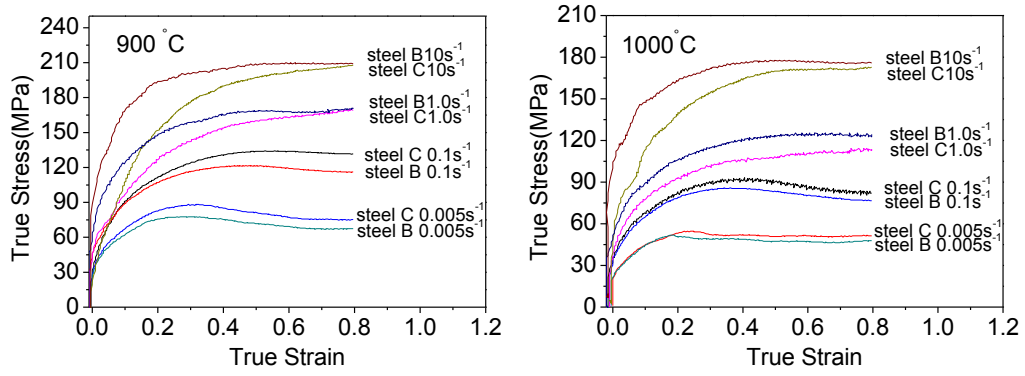


Fig. 2 Flow curves of steel B and steel C obtained at: (a) 900 °C; (b) 1000 °C.

Constitutive analysis

In order to investigate the effect of V and C on the hot flow behaviors of steel, it is necessary to study the constitutive characteristics. The effects of the temperature and strain rate on the deformation behaviors can be represented by Zener–Hollomon parameter, Z , in an exponent-type equation (Eq. (3)). The power law description of stress (Eq. (4)) is suitable for relatively low stresses when $\alpha\sigma < 0.8$, while the exponential law (Eq. (5)) is suitable for high stresses when $\alpha\sigma > 1.2$, and the hyperbolic sine law (Eq. (6)) is a more general form suitable for stresses over a wide range and gives better approximations between Z parameter and flow stress [13,14].

$$Z = \dot{\epsilon} \exp\left(\frac{Q}{RT}\right) \quad (3)$$

$$\dot{\epsilon} = A_1 \sigma^{n_1} \exp\left(\frac{-Q}{RT}\right) \quad (4)$$

$$\dot{\epsilon} = A_2 \exp(\beta\sigma) \exp\left(\frac{-Q}{RT}\right) \quad (5)$$

$$\dot{\epsilon} = A [\sinh(\alpha\sigma)]^n \exp\left(\frac{-Q}{RT}\right) \quad (6)$$

where $\dot{\epsilon}$ is the strain rate (s^{-1}), R is the universal gas constant ($8.3145 \text{ J mol}^{-1} \text{ K}^{-1}$), T is the absolute temperature (K), Q is the activation energy of hot deformation (J mol^{-1}), $A(A_1, A_2)$, α , β and $n(n_1)$ are the material constants, σ is the flow stress (MPa).

Using the methods depicted elsewhere [15,16,17], the hyperbolic sine constitutive equations of the three experimental steels were established using peak stress, and the parameters are shown in Table 3.

Table 3 The parameters in the hot deformation constitutive equations

Steels	w(C)/%	w(V)/%	α	n	$Q(\text{kJ/mol})$	$\ln A$
A	0.36	—	0.01	4.496	277.791	24.247
B	0.37	0.089	0.01	4.7721	280.554	24.20045
C	0.055	0.080	0.012	4.3396	287.599	23.454

The activation energy Q of hot deformation is a significant physical parameter, which serves as the indicator of deformation difficulty degree for plasticity deformation [18,19]. Table 4 lists the

activation energy of some C-Mn steels and microalloyed steels [4,20-23]. It is seen that alloy content has an important influence on hot deformation activation energy Q .

Table 4 The activation energy of some steels obtained by compression or torsion testing

Materials	Test	Deforming condition	Q (kJ/mol)	Ref
C-Mn	torsion	900-1100 °C, 0.5-6 s ⁻¹	276	[4]
C-Mn	compression	900-1100 °C, 0.005-10 s ⁻¹	278	This paper
C-Mn-0.043V	torsion	850-1100 °C, 0.5-6 s ⁻¹	275	[4]
C-Mn-0.060V	torsion	850-1100 °C, 0.5-6 s ⁻¹	278	[4]
C-Mn-0.093V	torsion	850-1100 °C, 0.5-6 s ⁻¹	279	[4]
C-Mn-0.089V	compression	900-1100 °C,0.005-10 s ⁻¹	281	This paper
C-Mn-Ti	compression	800-1200 °C, 0.2-50 s ⁻¹	312	[20]
C-Mn-Nb-Ti	compression	800-1200 °C, 0.2-50 s ⁻¹	325	[20]
C-Mn-Nb-Ti	compression	800-1150 °C,0.1-5 s ⁻¹	336	[21]
C-Mn-V-Cr-Ni	compression	850-1100 °C, 0.001-0.5 s ⁻¹	320	[22]
C-Mn-V-Ti	compression	900-1050°C,0.005-30 s ⁻¹	331	[23]

From Table 4, it is found that the activation energy of the experimental steel A and steel B is very close to the Q value of the C-Mn steel and vanadium microalloyed steels reported in literature [4], which is close to the self-diffusion activation energy of austenite. According to the Q value of the C-Mn steels and C-Mn-V steels, it is inferred that V addition in microalloyed steels seemed not to affect the activation energy much. The atomic radius of V is 1.34 Å, slightly greater than that of Fe (1.26 Å), and this may explain why its influence is practically nil for the low contents studied [4]. While the activation energy Q of other microalloyed steels listed in Table 4 is somewhat higher than the self-diffusion activation energy of austenite, this may be due to that these steels containing Nb, Ti, which can increase the activation energy dramatically [4], and some steels containing Cr, Ni, resulting in a strong solution dragging effect.

For the experimental steels, the activation energy Q about 288 kJ/mol for the steel C was slightly higher than that for the steel B (281 kJ/mol). It is supposed that C addition in vanadium microalloyed steels has the trend to reduce the hot deformation activation energy Q . The values for the activation energy obtained by other investigators are shown in Fig. 3. Medina et al. [4], Serajzadeh et al. [24] and Sakai et al. [25] have also reported that the activation energy decreased with increasing C content. Moreover, Mead et al. [26] have found that the activation energy for iron self-diffusion decreases with increasing C content.

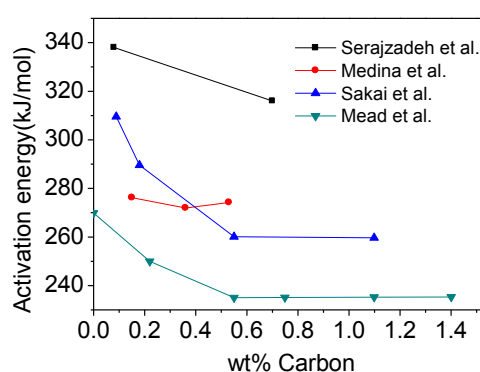


Fig. 3 The effect of C content on the activation energy for hot deformation and iron self diffusion reported before.

Characteristic points of flow curves

The strain hardening rate values ($\theta=d\sigma/d\varepsilon$) were plotted as a function of the flow stress at 0.1 s^{-1} and different temperatures for the three steels (Fig. 4). According to the approach of Jonas et al. [27], in the θ - σ curves the point at which the work hardening rate equals zero ($\theta=0$) represents the peak stress (σ_p), the inflection point of θ - σ curves indicates the critical stress (σ_c) for the initiation of DRX.

The dependence of the characteristic points of steels under different deformation conditions on Z parameter is shown in Fig. 5. It can be seen that the peak strain (stress) and the critical strain (stress) of the experimental steels increase with a higher Z parameter. Regression analysis of these curves resulted in the equations listed in Table 5.

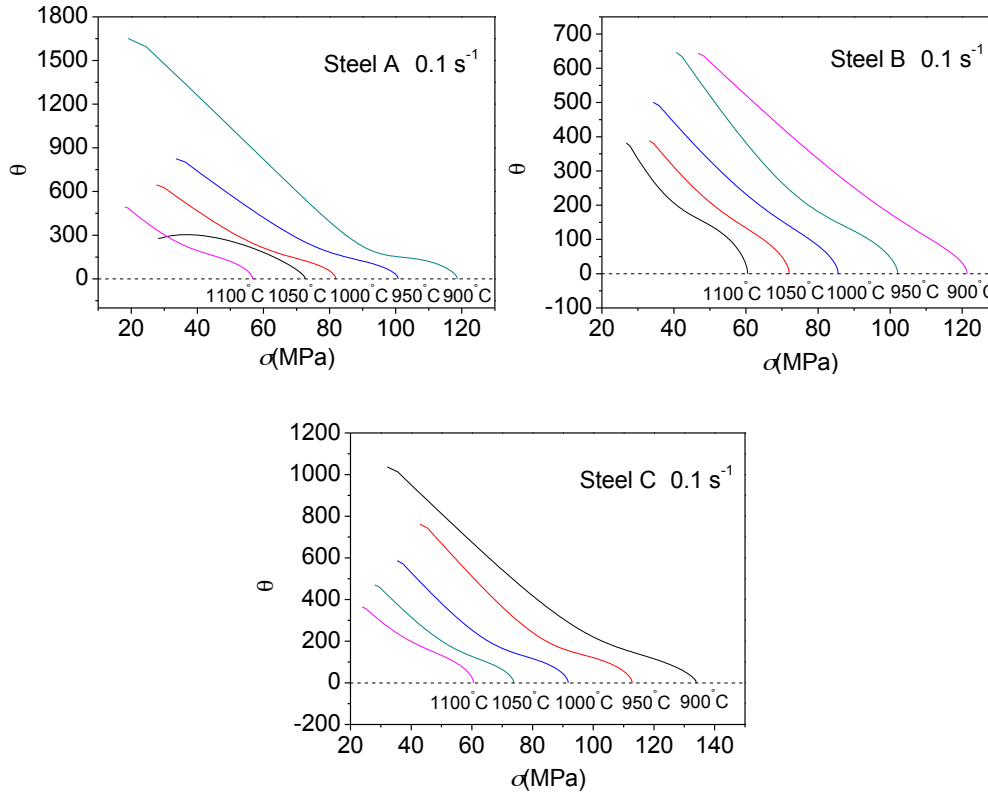


Fig. 4 Strain hardening rate (θ) versus true stress at 0.1 s^{-1} and different temperatures: (a) Steel A; (b) Steel B; (c) Steel C.

Table 5 The dependence of the characteristic points under different deformation conditions on Z parameter

	Steel A	Steel B	Steel C
$\ln\varepsilon_p - \ln Z$	$\ln\varepsilon_p = 0.14044 \ln Z - 4.45784$	$\ln\varepsilon_p = 0.1697 \ln Z - 5.17604$	$\ln\varepsilon_p = 0.15572 \ln Z - 4.86011$
$\ln\varepsilon_c - \ln Z$	$\ln\varepsilon_c = 0.15347 \ln Z - 5.72295$	$\ln\varepsilon_c = 0.18198 \ln Z - 6.45825$	$\ln\varepsilon_c = 0.1697 \ln Z - 5.17604$
$\ln\sigma_p - \ln Z$	$\ln\sigma_p = 0.1675 \ln Z + 0.34886$	$\ln\sigma_p = 0.16636 \ln Z + 0.40626$	$\ln\sigma_p = 0.17134 \ln Z + 0.22821$
$\ln\sigma_c - \ln Z$	$\ln\sigma_c = 0.19201 \ln Z - 0.46329$	$\ln\sigma_c = 0.19106 \ln Z - 0.38797$	$\ln\sigma_c = 0.18447 \ln Z - 0.29434$

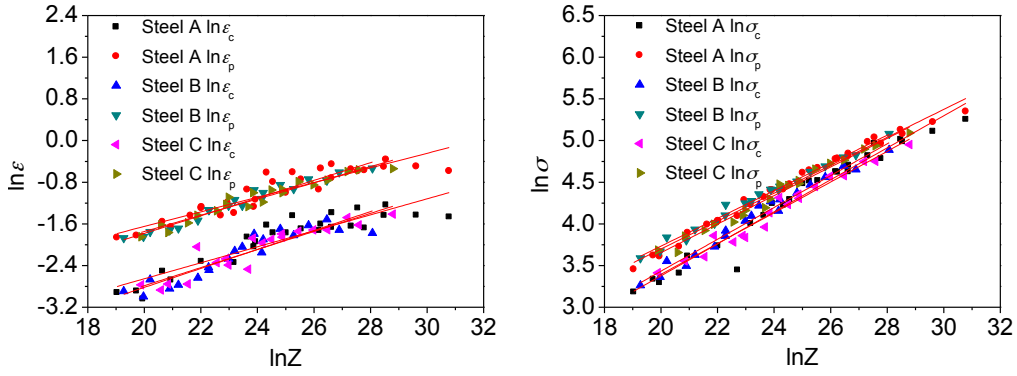


Fig. 5 Relationship between (a) ε_p , ε_c and Z ; (b) σ_p , σ_c and Z .

The relationship between ε_c (σ_c) and ε_p (σ_p) of steels is plotted in Fig. 6. It is seen that the dependence of ε_c (σ_c) on ε_p (σ_p) obeys a linear equation. Regression results of these curves are also shown in Fig. 6. It is also found that the ratio of ε_c to ε_p and σ_c to σ_p for the experimental steels are very close to each other.

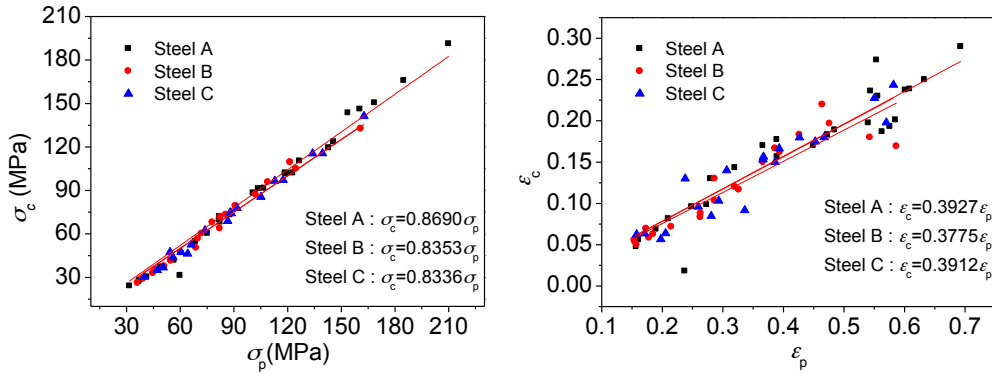


Fig. 6 Relationship between (a) ε_c and ε_p ; (b) σ_c and σ_p .

Effect of V and C on hot deformation flow stress

Fig. 7 and Fig. 8 show the variation of critical stress and peak stress with deformation temperatures and strain rates of the experimental steels, where the critical stresses and peak stresses are plotted as a function of the logarithm of the strain rate.

Fig. 7 shows the variation of critical stress and peak stress with deformation temperatures and strain rates of the steels A and B. From Fig. 7, it is seen more clearly that the critical stress and peak stress of steel B is higher than that of steel A under the same hot deformation conditions, which indicates that V micro alloying in steels offers beneficial effects as a solid solution strengthener and precipitation strengthener, which can increase the hot deformation flow resistance dramatically. In agreement, Medina et al. [4] investigated the hot deformation behavior of steels with different V content and drew the conclusion that V addition in steels can increase the flow stress.

Fig. 8 shows the variation of critical stress and peak stress with deformation temperatures and strain rates of the steels B and C. The range of strain rates in Fig. 8 is 0.005 - 0.5 s^{-1} . From Fig. 8, it is seen that the critical stress and peak stress of steel C is higher than that of steel B under the same hot deformation conditions.

The higher flow stress of steel C at lower strain rates (0.005 - 0.5 s^{-1} in this paper) indicates that C addition in vanadium microalloyed steel exhibits obvious softening effect, which is in reasonable agreement with some reports before [4,7]. Wray [7] confirmed that this behavior was attributed to a

decrease of the work hardening rate due to a relaxation of the crystallographic structure. Sherby [28] related the change in creep strength to the increase in self-diffusivity of iron with increasing C content and an increase in self-diffusivity is indicative of weaker interatomic bonding. And measurements before [29] showed that the austenitic-iron lattice is expanded by the addition of C. So it is inferred that the lower stress of steel B agrees with the reported increase in self-diffusivity and expansion of the austenite lattice with increasing C content.

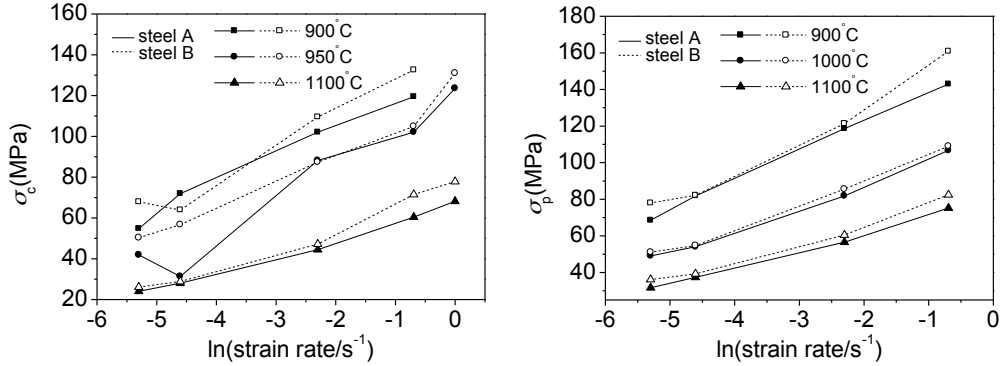


Fig. 7 Relationship between critical and peak stresses of steel A, steel B and the logarithm of the strain rate: (a) critical stress; (b) peak stress.

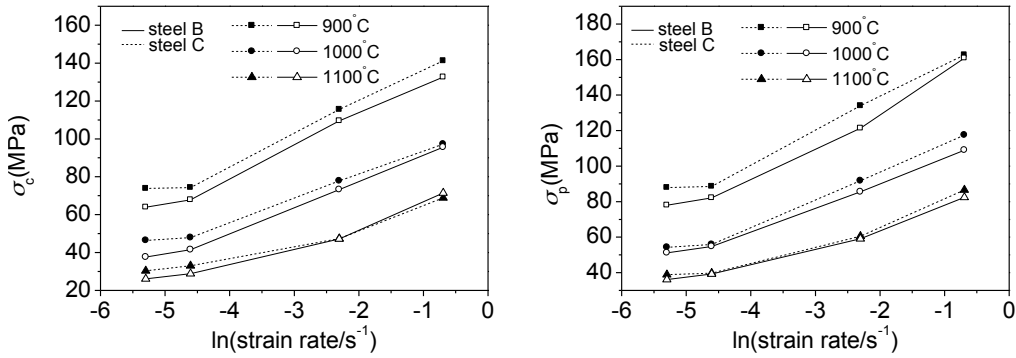


Fig. 8 Relationship between critical and peak stress of steel B, steel C and the logarithm of the strain rate: (a) critical stress; (b) peak stress.

However, from Fig. 2 we can see that when the strain rate increases to 1 and 10 s^{-1} , the steel B shows higher flow stress than the steel C, demonstrating that C addition in vanadium microalloyed steel has a hardening effect at higher strain rates (1-10 s^{-1} in this paper). It should be noted that for large Z parameter (i.e. high strain rates and/or low temperatures), DRX is postponed and the dominant softening mechanism would be only DRV. Additionally, at high strain rates the recovery process is controlled by cross slip process [30], and stacking fault energy is an important factor in controlling the cross slip of dislocations, a lower stacking fault energy causes a higher stress for cross slip. It is expected that under this condition, C addition increases the flow stress of steel due to its effect on reduction of stacking fault energy [30].

Effect of V and C on the peak strain of DRX

The peak strain ε_p is an important parameter. The critical strain ε_c at which DRX begins can be approximately determined by the peak strain ε_p [31]. The variation of peak strain with deformation temperatures and strain rates of the steel A and steel B is shown in Fig. 9, where the peak strain is plotted as a function of the logarithm of the strain rate. It is worth mentioning that some curves show

deviation from theoretical values. This is associated with experimental error and the noise level of the experimental data. Although such noise was relatively low, it was effective enough to cause a large spread during the data processing involved in the differentiating stages.

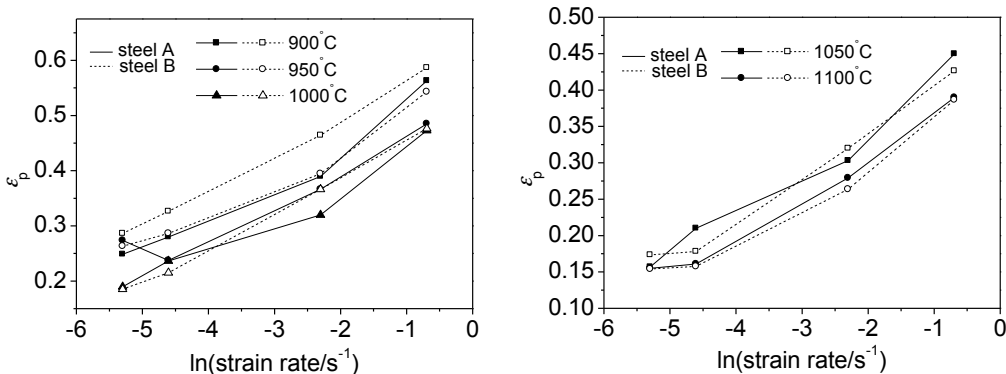


Fig. 9 Relationship between peak strain and the logarithm of the strain rate for steel A and steel B: (a) 900 °C-1000 °C; (b) 1050 °C-1100 °C.

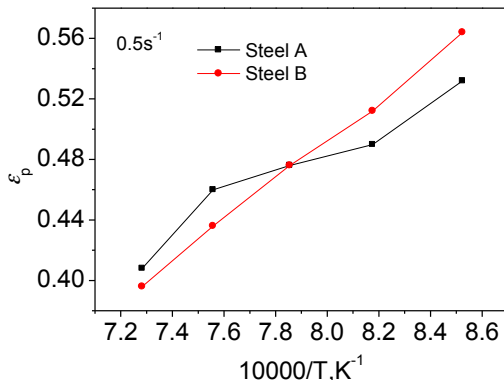


Fig. 10 Peak strain as a function of the inverse absolute temperature at strain rate of 0.5 s^{-1} for steel A and steel B

From Fig. 9, we can see that the peak strain of steel B is higher than that of steel A under lower temperatures (900-1000 °C), while at higher temperatures (1050-1100 °C), the peak strain of steel B is lower than that of steel A. The variation of peak strain with deformation temperatures can be seen more clearly in Fig. 10, where the peak strain at the strain rate of 0.5 s^{-1} is plotted as a function of the deformation temperatures. The higher peak strain of steel B under lower temperatures may due to the solute drag effect of V and the dynamic precipitation pinning effect of V(C,N) during deformation, which can inhibit the onset of DRX and lead to higher peak strain. While at higher temperatures, dynamic precipitation of steel B is unable to occur as seen in Table 2, and due to the coarser prior austenite grain size of steel A, which means less grain boundaries, namely, the prior nucleation sites for DRX, so the nucleation of DRX is inhibited in steel A, leads to higher peak strain. Therefore, it is inferred that V addition in steels influence the onset of DRX through solute drag effect and dynamic precipitation pinning effect, which can inhibit the onset of DRX, while V addition can also refine the prior austenite grain size, which can accelerate the occurrence of DRX.

The variation of peak strain with deformation temperatures and strain rates of the steel B and steel C is shown in Fig. 11. From Fig. 11, it is seen clearly that the peak strain of steel C is higher than that of the steel B, which indicates that C addition promote the occurrence of DRX. In

agreement, research works [11,32,33,34] before have shown that interstitial alloying elements like carbon and boron can accelerate the onset of the DRX.

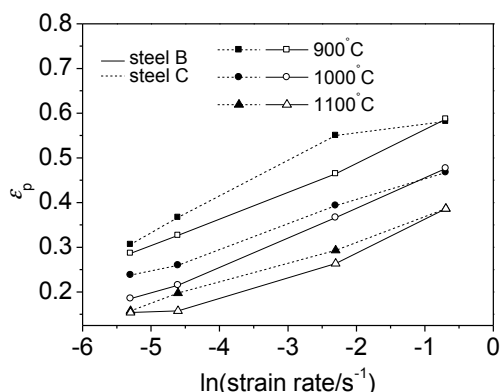


Fig. 11 Relationship between peak strain and the logarithm of the strain rate for steel B and steel C

CONCLUSIONS

The hot flow behaviors of a C-Mn steel (0.36C-1.42Mn) and two V microalloyed steels (0.37C-1.46Mn-0.089V and 0.055C-1.45Mn-0.080V) have been investigated at the temperatures from 900 °C to 1100 °C and strain rates from 0.005 s⁻¹ to 10 s⁻¹, the main results are as follows:

(1) V addition in steels can effectively increase the flow stress. Increasing the C content of vanadium microalloyed steel decreases the flow stress at lower strain rates, whilst at higher strain rates C addition leads to higher flow stress.

(2) The flow stress constitutive equations of hot deformation for the three steels were developed. Results showed that V has little effect on hot deformation activation energy Q , while increasing the C content of vanadium microalloyed steel has the trend to reduce the hot deformation activation energy.

(3) V addition can influence the occurrence of dynamic recrystallization through complex interaction of solute drag effect, dynamic precipitate pinning effect and its refining effect on prior austenite grain size, while C addition promotes the occurrence of dynamic recrystallization.

ACKNOWLEDGES

This study was financially supported by the National Natural Science Foundation of China (No. 51071019 and No. 51371030) and National High Technology Research and Development Program of China (No. 2013AA031601).

REFERENCES

- [1] J.M. Cabrera, A. Al. Omar, J.M. Prado, J.J. Jonas, *Metall. Mater. Trans. A* 28 (1997) 2233-2244.
- [2] D.J. Naylor, *Ironmak. Steelmak.* 16 (1989) 246-252.
- [3] F.B.El. Hassani, A. Chenaouia, R. Dkiouak, *J. Mater. Proc. Tech.* 199 (2008) 140-149.
- [4] S.F. Medina, C.A. Hernandez, *Acta mater.* 44 (1996)137-148.
- [5] S.F. Medina, C.A. Hernandez, *Acta mater.* 44 (1996)149-154.
- [6] J.B. Wu, G.Q. Liu, H. Wang, *Acta metall. sin.* 46(2010)838-843.
- [7] P.J. Wray, *Metall. Trans. A* 13 (1982) 125-134.
- [8] H. Beladi, P.D. Hodgson, *Scr. Mater.* 56 (2007) 1059-1062.
- [9] L.X. Kong, P.D. Hodgson, D.C. Collinson, *ISIJ Int.* 38 (1998) 1121-1129.
- [10] S. Serajzadeh, A. Karimi Taheri, *Mech. Mater.* 35 (2003) 653-660.
- [11] F. Escobar, J.M. Cabrera, J.M. Prado, *Mater. Sci. Tech.* 19 (2003) 1137-1147.
- [12] T. Gladman, D. Dulieu, McIvor, *Microalloying 75*, Union Carbide, New York, 1977, p. 23.
- [13] H. Mirzadeh, J.M. Cabrera, J.M. Prado, A. Najafzadeh, *Mater. Sci. Eng. A* 528 (2011)

3876-3882.

- [14] M. Meysami, S.A.A.A. Mousavi, *Mater. Sci. Eng. A* 528 (2011) 3049-3055.
- [15] H.L. Wei, G.Q. Liu, X. Xiao, H.T. Zhao, H. Ding, R.M. Kang, *Mater. Sci. Eng. A* 564 (2013) 140-146.
- [16] H.L. Wei, G.Q. Liu, X. Xiao, M.H. Zhang, *Mater. Sci. Eng. A* 573(2013) 215-221.
- [17] H.L. Wei, G.Q. Liu, H.T. Zhao, R.M. Kang, *Mater. Des.* 50 (2013) 484-490.
- [18] N.P. Jin, H. Zhang, Y. Han, W.X. Wu, J.H. Chen, *Mater. Charact.* 60 (2009) 530-536.
- [19] M.R. Rokni, A. Zarei-Hanzaki, A.A. Roostaei, A. Abolhasani, *Mater. Des.* 32 (2011) 4955-4960.
- [20] A. Laasraoui, J.J. Jonas, *Metall. Mater. Trans. A* 22(1991)1545-1558.
- [21] L.Y. Lan, C.L. Qiu, D.W. Zhao, X.H. Gao, L.X. Du, *J. Iron Steel Res. Int.* 18(2011)55-60.
- [22] M. Meysami, S.A.A.A. Mousavi, *Mater. Sci. Eng. A* 528(2011) 3049-3055.
- [23] C.Y. Wang, G.Q. Liu, J.B. Wu, L. Xu, *Heat Treat. Met.* 35(2010)33-36(in chinese).
- [24] S. Serajzadeh, A. Karimi Taheri, *Mater. Des.* 23 (2002) 271-276.
- [25] T. Sakai, M. Ohasi, *Tetsu-to-Hagané* 67 (1981) 2000-2009.
- [26] H.W. Mead, C.E. Birchenall, *J. Met.* 8 (1956) 1336-1339.
- [27] J.J. Jonas, X. Queleñec, L. Jiang, E. Martin, *Acta Mater.* 57 (2009) 2748-2756.
- [28] O.D. Sherby, *Acta Metall.* 10 (1962) 135-147.
- [29] N. Ridley, H. Stuart, *Met. Sci.* 4 (1970) 219-222.
- [30] R.W.K. Honeycombe, H.K.D.H. Bhadeshia, *Steels: Microstructure and Properties*, Edward Arnold, London, UK, 1981.
- [31] B.X. Wang, X.H. Liu, G.D. Wang, *Mater. Sci. Eng. A* 393 (2005) 102-108.
- [32] Z. Xu, G.R. Zhang, T. Sakai, *ISIJ Int.* 35 (1995) 210-216.
- [33] E. López-Chipres, I. Mejía, C. Maldonado, A. Bedolla-Jacuinde, M. El-Wahabi, J.M. Cabrera, *Mater. Sci. Eng. A* 480 (2008) 49-55.
- [34] I. Mejía, A. Bedolla-Jacuinde, C. Maldonado, J.M. Cabrera, *Mater. Sci. Eng. A* 528 (2011) 4133-4140.